Video Article

High Temperature Fabrication of Nanostructured Yttria-Stabilized-Zirconia (YSZ) Scaffolds by *In Situ* Carbon Templating Xerogels

Sixbert P. Muhoza[1], Matthew A. Cottam[1], Michael D. Gross[1,2]

[1]Department of Chemistry, Wake Forest University

[2]Center for Energy, Environment, and Sustainability, Wake Forest University

Correspondence to: Michael D. Gross at grossmd@wfu.edu

URL: https://www.jove.com/video/55500
DOI: doi:10.3791/55500

Keywords: Engineering, Issue 122, solid oxide fuel cell, yttria stabilized zirconia, *in-situ* carbon templating, xerogel, porous, composite, nanostructure

Date Published: 4/16/2017

Citation: Muhoza, S.P., Cottam, M.A., Gross, M.D. High Temperature Fabrication of Nanostructured Yttria-Stabilized-Zirconia (YSZ) Scaffolds by *In Situ* Carbon Templating Xerogels. *J. Vis. Exp.* (122), e55500, doi:10.3791/55500 (2017).

Abstract

We demonstrate a method for the high temperature fabrication of porous, nanostructured yttria-stabilized-zirconia (YSZ, 8 mol% yttria - 92 mol% zirconia) scaffolds with tunable specific surface areas up to 80 $m^2 \cdot g^{-1}$. An aqueous solution of a zirconium salt, yttrium salt, and glucose is mixed with propylene oxide (PO) to form a gel. The gel is dried under ambient conditions to form a xerogel. The xerogel is pressed into pellets and then sintered in an argon atmosphere. During sintering, a YSZ ceramic phase forms and the organic components decompose, leaving behind amorphous carbon. The carbon formed *in situ* serves as a hard template, preserving a high surface area YSZ nanomorphology at sintering temperature. The carbon is subsequently removed by oxidation in air at low temperature, resulting in a porous, nanostructured YSZ scaffold. The concentration of the carbon template and the final scaffold surface area can be systematically tuned by varying the glucose concentration in the gel synthesis. The carbon template concentration was quantified using thermogravimetric analysis (TGA), the surface area and pore size distribution was determined by physical adsorption measurements, and the morphology was characterized using scanning electron microscopy (SEM). Phase purity and crystallite size was determined using X-ray diffraction (XRD). This fabrication approach provides a novel, flexible platform for realizing unprecedented scaffold surface areas and nanomorphologies for ceramic-based electrochemical energy conversion applications, *e.g.* solid oxide fuel cell (SOFC) electrodes.

Video Link

The video component of this article can be found at https://www.jove.com/video/55500/

Introduction

The solid oxide fuel cell (SOFC) holds great promise as an alternative energy conversion technology for the efficient generation of clean electrical power.[1] Considerable progress has been made in the research and development of this technology; however, improvements in electrode performance are still needed to achieve reliable commercialization. The electrode often comprises a porous ceramic scaffold with electrocatalytic particles decorated on the scaffold surface. A large body of research has focused on increasing the surface area of the electrocatalytic particles to increase performance,[2,3,4,5,6,7,8] but there is very little research on increasing the scaffold surface area. Increasing the scaffold surface area is challenging because they are sintered at high temperatures, 1,100 °C to 1,500 °C.

Scaffolds processed by traditional sintering typically have a specific surface area of 0.1-1 $m^2 \cdot g^{-1}$.[8,9,10,11] There are a few reports on increasing the scaffold surface area. In one case, the surface area of a traditionally sintered scaffold was enhanced by dissolution and precipitation of the scaffold surface using hydrofluoric acid, achieving a specific surface area of 2 $m^2 \cdot g^{-1}$.[12] In another, high temperatures were avoided altogether by using pulsed laser deposition, achieving a specific surface area of 20 $m^2 \cdot g^{-1}$.[13] The rationale behind the development of our technique was to create a low cost fabrication process that provides unprecedented scaffold surface areas and uses traditional sintering temperatures so that the process can be adopted easily. With the technique reported here, scaffold surface areas up to 80 $m^2 \cdot g^{-1}$ have been demonstrated while being processed at traditional sintering temperatures.[14]

Our research is primarily motivated by SOFC electrode engineering, but the technique is more broadly applicable to other fields and applications. Generally, the *in situ* carbon templating method is a flexible approach that can produce nanostructured, high surface area mixed-metal ceramic materials in the powder or porous scaffold form. It is flexible in that the mixed-metal ceramic composition, surface area, porosity, and pore size can all be tuned systematically. High temperatures are often needed to form the desired phase in mixed-metal ceramics, and this approach preserves ceramic nanomorphology while allowing one to choose essentially any processing temperature.

This method involves the synthesis of a hybrid inorganic-organic propylene-oxide-based gel, with a well define stoichiometry of metal ions and ratio of inorganic to organic content. The gel is dried under ambient conditions to form a xerogel. The xerogel is sintered in an argon atmosphere at the desired temperature. Upon heating, the organic component decomposes leaving behind a carbon template *in situ*, which remains for

the duration of sintering. The carbon template is subsequently removed by low temperature oxidation in air, resulting in a nanostructured, high surface area ceramic.

Protocol

1. Preparing Xerogel Pellets

1. Gel Synthesis
    1. Add a 25 mm magnetic stir bar and 113 mL of deionized water to a 500 mL beaker. Magnetically stir the deionized water at the highest rate that does not form a vortex.
    2. Slowly add 13.05 g (0.056 mol) of anhydrous zirconium chloride to the deionized water in small increments. After all of the anhydrous zirconium chloride has dissolved, add 53.29 g (0.296 mol) of glucose to the solution.
    3. After all of the glucose has dissolved in the solution, add 3.73 g (0.01 mol) of yttrium nitrate hexahydrate to the solution. Increase the rate of magnetic stirring to ~700 rpm and wait for all of the yttrium nitrate hexahydrate to dissolve in solution.
    4. Add 42 mL of propylene oxide to the solution. Continue stirring at ~700 rpm for the propylene oxide to mix with the aqueous solution. Once the propylene oxide is mixed with the aqueous solution (~10 s), decrease the magnetic stirring to ~150 rpm.
    5. Continue stirring until the magnetic stir bar has stopped moving due to formation of the gel. The gel typically forms within 3 min.
    NOTES: Adding anhydrous zirconium chloride to deionized water is a highly exothermic reaction and the anhydrous zirconium chloride will plume if it is added too quickly.
    The formulation provided in Section 1.1. corresponds to a glucose to total metals (zirconium + yttrium) molar ratio of 4.5:1. The representative results section includes data for glucose to total metals molar ratios of 0:1, 2.25:1, and 4.5:1. The amount of glucose in the formulation is only limited by the solubility of glucose in the solution. For reference, the maximum solubility of glucose in water at 20 °C is 47.8 wt%.[15]

2. Aging and Washing the Gel
    1. Tightly cover the beaker containing the gel with Parafilm and let it age for 24 h by leaving the covered beaker at room temperature.
    2. Remove the cover from the beaker and decant the liquid on top of the gel.
    3. Add 300 mL of absolute ethanol to the beaker containing the gel, tightly cover the beaker with Parafilm, and leave the covered beaker at room temperature for 24 h.
    4. Repeat step 1.2.3 two more times for a total of three ethanol washings over a total period of 72 h.

3. Drying the Gel into a Xerogel
    1. Remove the gel from the beaker and place it in a 2 L porcelain evaporating dish (24 cm outside top diameter) using a laboratory spatula.
    2. Break the gel into approximately 1 cm x 1 cm pieces with a spatula and spread out the pieces over the surface of the evaporating dish.
    3. Let the gel pieces dry under ambient conditions for one week or until the gel is dry. The gel is considered dry when it can be ground into a fine powder.
    4. Grind all of the xerogel into a fine powder with a mortar and pestle.
    NOTE: Once the gel is dry, it is considered a xerogel because it was dried under ambient conditions.

4. Pressing the Xerogel into a Pellet
    1. Place 1 g of xerogel powder into a cylindrical pellet press die with a diameter of 13 mm.
    2. Using a hydraulic press, apply 22 kN of force for 90 s to press the xerogel gel into a pellet.
    3. Slowly release the force applied by the press. Slowly eject the pellet out of the pellet die and then carefully remove the pellet.

2. Sintering the Xerogel Pellet in an Inert Atmosphere

1. Place the xerogel pellet onto an alumina or yttria-stabilized zirconia plate and load the plate into the center of a tube furnace.
2. Flow argon at a rate of one third the volume of the working tube per minute. This corresponds to an argon flow rate of 750 mL·min^{-1} for the working tube used in this work. Vent the gas outlet to a fume hood.
3. Flow argon for at least 15 min before starting to heat the tube furnace.
4. While continuously flowing argon at a constant rate, program the tube furnace temperature controller to the following heating schedule:
    1. Hold at room temperature for 15 min.
    2. Heat to 850 °C at a ramp rate of 5 °C·min^{-1}.
    3. Heat to desired sintering temperature at a ramp rate of 2 °C·min^{-1}.
    4. Hold at the desired sintering temperature for 2 h.
    5. Cool to 850 °C at a ramp rate of 2 °C·min^{-1}.
    6. Cool to room temperature at a ramp rate of 5 °C·min^{-1}.
5. Start the program and double-check that the tube furnace is heating up following the schedule provided in section 2.3.
6. Remove pellet from the tube furnace after the heating program has completed.

3. Determining Carbon Template Concentration

1. Cut a ~50 mg piece out of the sintered xerogel pellet with a utility knife and grind it into a fine powder with an agate mortar and pestle.
2. Place ~50 mg of the fine powder into an alumina sample cup for thermogravimetric analysis.

3. Using a thermogravimetric analyzer (TGA), heat the sample at a rate of 10 °C·min^{-1} from ambient temperature to 1,200 °C while flowing air over the sample at a rate of 100 mL·min^{-1}.
4. Calculate the percent change in weight that occurs between ~350 °C and ~700 °C. This weight percent corresponds to the total carbon content in the sample.
   NOTE: If a weight increase occurs in the 350 °C to 700 °C range, a carbide phase has formed and the calculation of carbon content is more complex. For this case, please refer to calculations described in the literature.[14] Carbon elemental analysis has been used to confirm that carbon content can be calculated from TGA measurements.

4. Preparing High Surface Area YSZ Scaffold by Carbon Template Removal

1. Place the sintered xerogel pellet in an alumina crucible.
2. Place the crucible into a box furnace at 700 °C for 2 h.
3. Carefully remove the hot crucible from the box furnace with stainless steel crucible tongs and allow it to cool to room temperature for one hour before removing the porous, white YSZ scaffold.

Representative Results

Phase purity was confirmed by X-ray diffraction (XRD) as previously reported by Cottam *et al.*[14] YSZ scaffold specific surface area as a function of carbon template concentration is shown in **Figure 1**. The concentration is shown as the volume percent of total solids in the sintered xerogel pellet. The carbon template concentration systematically increases with increasing glucose concentration in the gel formulation. As shown in **Figure 1**, the specific surface area systematically increases from 10 $m^2 \cdot g^{-1}$ to 68 $m^2 \cdot g^{-1}$ by increasing the glucose:metals molar ratio from 0:1 to 4.5:1.

The carbon template concentration was quantified using TGA (**Figure 2**). The carbon template concentration was 4 wt% and 64 wt% of total solids for glucose:metals molar ratios of 0:1 and 4.5:1. A YSZ density of 5.9 $g \cdot cm^3$ and a carbon density of 2.15 $g \cdot cm^3$ were used to convert between weight percent and volume percent.

Figure 3 shows scanning electron microscopy (SEM) images of the YSZ xerogel with and without the glucose additive. Both samples were similarly sintered at 1,150 °C in argon and burned out in air at 700 °C. The particles of YSZ xerogel with glucose additive are several times smaller than those without glucose additive. The formation of smaller particles by adding glucose to the gel is consistent with their high carbon content and surface area.

Figure 4 shows XRD patterns of the strongest YSZ peak for YSZ scaffolds as a function of glucose:metals molar ratio. The crystallite size was calculated using these peaks and the Scherrer equation. The crystallite size decreased from 22 nm to 12 nm to 9 nm as the glucose:metals molar ratio was increased from 0:1 to 2.25:1 to 4.5:1. The crystallite size progression is consistent with the observed increase in surface area with increasing glucose:metals molar ratio.

Figure 5 shows the YSZ scaffold pore size distribution as a function of glucose:metals molar ratio. The adsorption/desorption data was collected with a physical adsorption instrument, which is limited to calculating pore sizes between 2 nm and 14 nm. The pore size distribution calculated from N_2 adsorption data is shown in **Figure 5a**. Only the 2.25:1 glucose:metals molar ratio data shows a maximum. Since the instrumentation was limited to detecting 14 nm pores, pore size distributions from N_2 desorption data were also calculated, **Figure 5b**. Desorption data tends to show "artificially" narrow pore size distributions and "artificially" smaller pores[16]; however, the desorption data provides more insight into the progression of pore size distribution than the adsorption data. The differences in pore size distribution for adsorption and desorption data is best compared for the 2.25:1 glucose:metals data in **Figure 5**. The peak of the pore size distribution shifts from 10 nm to 7 nm and the distribution is narrower. Extrapolating to the 4.5:1 data, it seems reasonable to assume the peak of the pore size distribution is in the 16-20 nm range. Overall, **Figure 5** shows both the number of pores and size of pores increase with an increase in glucose:metals molar ratio.

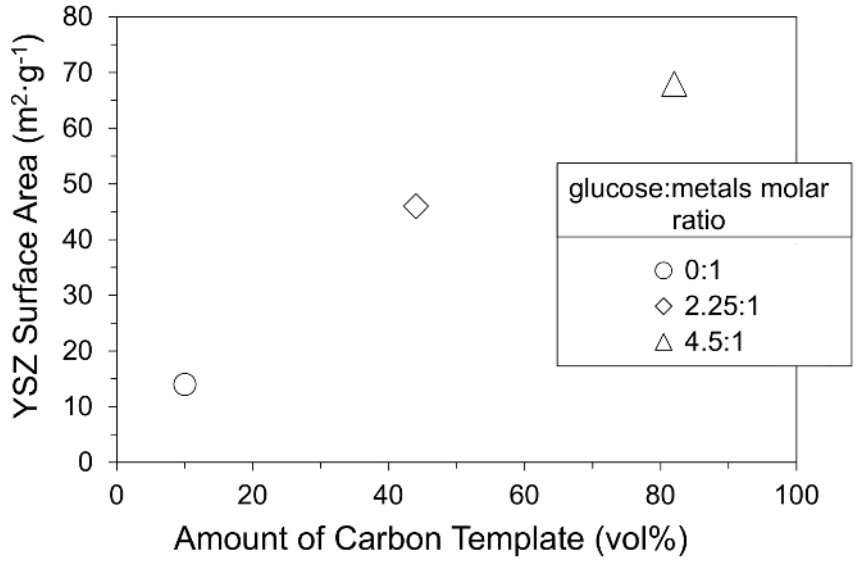

Figure 1: YSZ scaffold surface area as a function of carbon template concentration and glucose:metals molar ratio. Please click here to view a larger version of this figure.

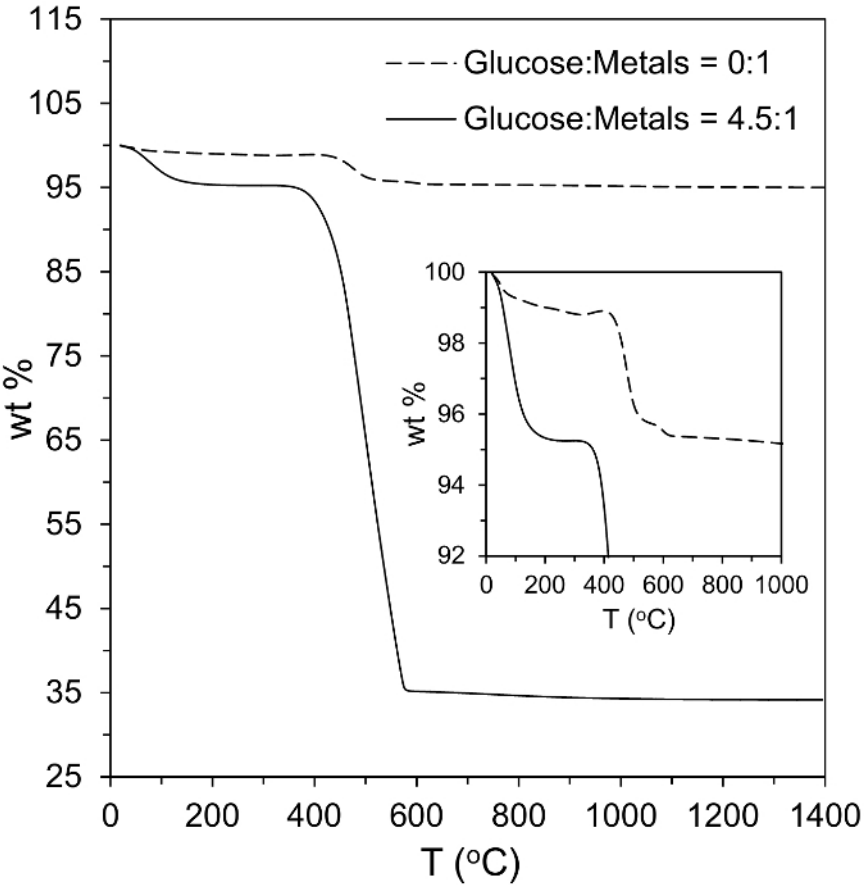

Figure 2: TGA curves in flowing air for xerogels with glucose:metal molar ratios of 0:1 and 4.5:1 sintered at 1,150 °C in argon for 2 h. Please click here to view a larger version of this figure.

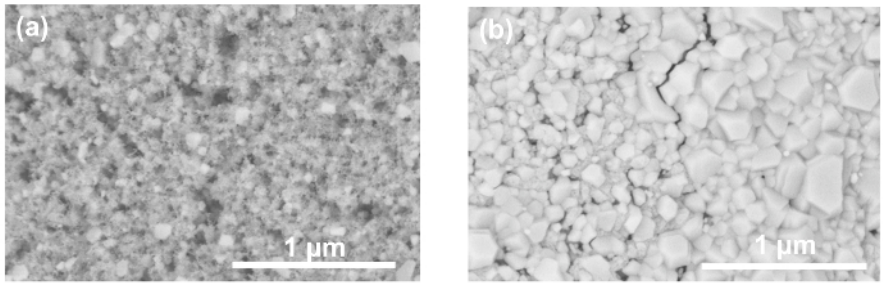

Figure 3: SEM micrographs of YSZ scaffolds for glucose:metals molar ratios of (**a**) 4.5:1 and (**b**) 0:1. The xerogels were sintered in argon at 1,150 °C for 2 h and then heated in air at 700 °C. Please click here to view a larger version of this figure.

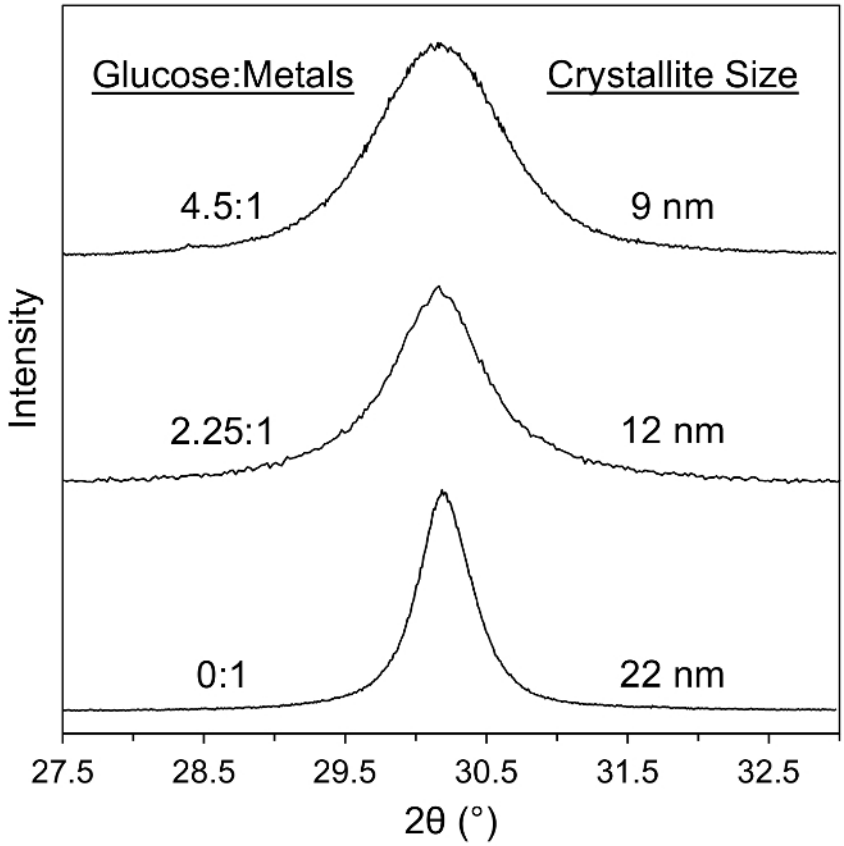

Figure 4: XRD of strongest YSZ peak for YSZ scaffolds as a function of glucose:metals molar ratio. Please click here to view a larger version of this figure.

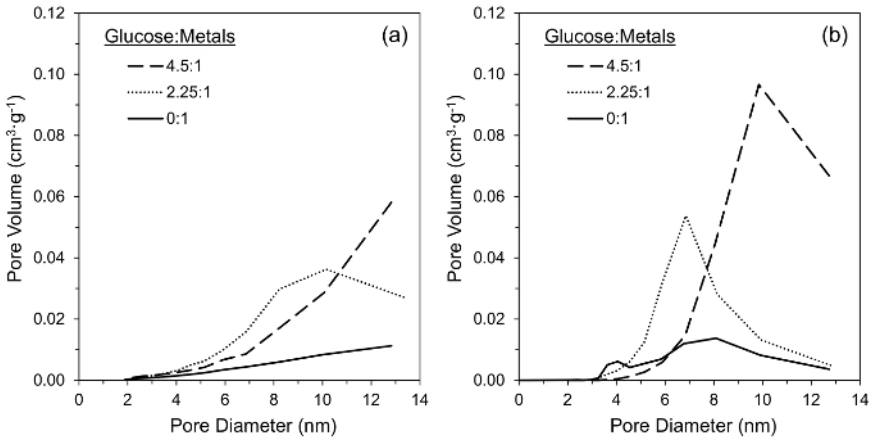

Figure 5: YSZ scaffold Dollimore-Heal pore size distribution as a function of glucose:metals molar ratio calculated from (**a**) N_2 adsorption data and (**b**) N_2 desorption data. Please click here to view a larger version of this figure.

Discussion

With this *in situ* carbon templating approach, one can create and preserve nanomorphology in mixed-metal-oxides at traditional ceramic scaffold sintering temperatures. The resulting surface areas are up to 80 times higher than traditionally sintered scaffolds and up to 4 times higher than scaffolds fabricated by complex deposition techniques.[14] The propylene oxide-glucose gel system is highly flexible for tuning the concentration of the carbon template, allowing one to systematically control the carbon template concentration between 10 vol% carbon and virtually 100 vol% carbon.

There are three critical steps to the procedure. First, the propylene oxide must be well mixed with the aqueous solution to form the gel (Step 1.1.4). This is accomplished by stirring at ~700 rpm while the propylene oxide is added. If the solution is not stirred turbulently, the propylene oxide will form a separate layer above the aqueous solution and the gel will not form. Second, the working tube must be flushed with argon before heating the tube furnace for sintering (Step 2.2). This is accomplished by flowing argon for 15 min at a rate of one third the volume of the working tube per minute. In addition, the working tube must be leak tight to prevent air from entering the working tube during sintering. Oxygen from the air will destroy the carbon template by oxidation of carbon to carbon dioxide. Third, the sintering ramp rate from 850 °C to sintering temperature should not exceed 2 °C·min^{-1}. A faster ramp rate could cause the scaffold to fracture.

The majority of possible carbon template concentrations will result in a monolithic scaffold. Obviously, there is a critical carbon concentration threshold at which a monolithic scaffold will not form because the YSZ particles would be disconnected from each other. However, this scenario also has utility. One could load a traditional low surface area scaffold with a high carbon concentration gel and carry out the same inert sintering procedure described here. The result would be YSZ nanoparticles decorated onto the scaffold surface in a nanoparticle concentration controlled by the glucose concentration in the gel formulation.

Propylene oxide gel syntheses have been reported for a large number of metals in the literature.[17,18,19] In addition, the propylene oxide gel synthesis can accommodate multiple metals in essentially any mixed-metal composition that is desired. While the motivation for this work was driven by solid oxide fuel cell electrode needs, the approach is applicable for a wide range of mixed-metal-oxides for a wide range of applications.

It is important to recognize that if the sintering temperature is high enough, metal-carbide phases will form, rather than the oxide. The temperature at which this happens depends on the specific metals one is using. For YSZ, we have found that a zirconium carbide phase begins to form around 1,150 °C and nearly all of the zirconium is in the form of zirconium carbide by 1,400 °C.[14] For sintering temperatures below 1,300 °C, all of the zirconium reverts back to the YSZ phase upon carbon template removal by oxidation. For sintering temperatures above 1,300 °C, we observe small amounts of a monoclinic zirconium oxide phase. It is likely that above 1,300 °C, some zirconium carbide particles are sufficiently separated from yttrium such that heating in air to 700 °C is not enough thermal energy for complete dissolution of zirconium back into YSZ. Our group is currently considering alternative sintering environments to mitigate carbide formation while preserving the carbon template during sintering.

In summary, the propylene oxide-glucose gel system has outstanding flexibility in specifying the inorganic:organic ratio, the type of metals, and the mixed-metal composition for realizing high surface area mixed-metal-oxide nanomorphologies at high temperatures.

Disclosures

We have nothing to disclose.

Acknowledgements

This work was supported by the Wake Forest Chemistry Department and the Wake Forest Center for Energy, Environment, and Sustainability (CEES). We thank Charles Mooney and the Analytical Instrumentation Facility of the North Carolina State University for assistance with SEM imaging.

References

1. Badwal, S.P.S., Giddey, S.S., Munnings, C., Bhatt, A.I., & Hollenkamp, A.F. Emerging electrochemical energy conversion and storage technologies. *Front. Chem.* **2** (79), 1-28 (2014).
2. Gross, M.D., Vohs, J.M., & Gorte, R.J. An examination of SOFC anode functional layers based on ceria in YSZ. *J. Electrochem. Soc.* **154** (7), B694-B699 (2007).
3. Smith, B.H., & Gross M.D. A highly conductive oxide anode for solid oxide fuel cells. *Electrochem. Solid-State Lett.* **14** (1), B1-B5 (2011).
4. Vo, N.M., & Gross, M.D. The effect of vanadium deficiency on the stability of Pd and Pt catalysts in lanthanum strontium vanadate solid oxide fuel cell anodes. *J. Electrochem. Soc.* **159** (5), B641-B646 (2012).
5. Sholklapper, T.Z., Jacobson, C.P., Visco, S.J., & De Jonghe, L.C. Synthesis of dispersed and contiguous nanoparticles in solid oxide fuel cell electrodes. *Fuel Cells.* **8** (5), 303-312 (2008).
6. Jiang, Z., Xia, C., & Chen, F. Nano-structured composite cathodes for intermediate-temperature solid oxide fuel cells via an infiltration/impregnation technique. *Electrochim. Acta.* **55** (11), 3595-3605 (2010).
7. Zhan, Z., Bierschenk, D.M., Cronin, J.S., & Barnett, S.A. A reduced temperature solid oxide fuel cell with nanostructured anodes. *Energy Environ. Sci.* **4**, 3951-3954 (2011).
8. Gross, M.D., Vohs, J.M., & Gorte, R.J. Recent progress in SOFC anodes for direct utilization of hydrocarbons. *J. Mater. Chem.* **17**, 3071-3077 (2007).
9. Gross, M.D., Carver, K.M., Deighan, M.A., Schenkel, A., Smith, B.M., & Yee A.Z. Redox stability of $SrNb_xTi_{1-x}O_3$-YSZ for use in SOFC anodes. *J. Electrochem. Soc.* **156** (4), B540-B545 (2009).
10. Savaniu, C.D., & Irvine, J.T.S. La-doped $SrTiO_3$ as anode material for IT-SOFC. *Solid State Ionics.* **192** (1), 491-493 (2011).
11. Choi, S., Shin, J., & Kim, G. The electrochemical and thermodynamic characterization of $PrBaCo_{2-x}Fe_xO_{5+\delta}$ (x=0,0.5,1) infiltrated into yttria-stabilized zirconia scaffold as cathodes for solid oxide fuel cells. *J. Power Sources.* **201**, 10-17 (2012).
12. Kungas, R., Kim, J-S., Vohs, J.M., & Gorte, R.J. Restructuring porous YSZ by treatment in hydrofluoric acid for use in SOFC cathodes. *J. Am. Ceram. Soc.* **94** (7), 2220-2224 (2011).
13. Jung, W, Dereux, J.O., Chueh, W.C., Hao, Y., & Haile, S.M. High electrode activity of nanostructured, columnar ceria films for solid oxide fuel cells. *Energy Environ. Sci.* **5**, 8682-8689 (2012).
14. Cottam, M., Muhoza, S., & Gross, M.D. Preserving nanomorphology in YSZ scaffolds at high temperatures via in situ carbon templating of hybrid materials. *J. Amer. Ceram. Soc.* **99** (8), 2625-2631 (2016).
15. Alves, L.A., Silva J.B.A., & Giulietti, M. Solubility of D-Glucose in Water and Ethanol/Water Mixtures. *J. Chem. Eng. Data.* **52**, 2166-2170 (2007).
16. Thommes, M., Smarsly, B., Groenewolt, M., Ravikovitch, P.I., & Neimark, A.V. Adsorption hysteresis of nitrogen and argon in pore networks and characterization of novel micro- and mesoporous silicas. *Langmuir.* **22**, 756-764 (2006).
17. Chervin, C.N., *et al.* A non-alkoxide sol-gel method for the preparation of homogeneous nanocrystalline powders of $La_{0.85}Sr_{0.15}MnO_3$. *Chem. Mater.* **18**, 1928-1937 (2006).
18. Clapsaddle, B.J., Sprehn, D.W., Gash, A.E., Satcher Jr., J.H., & Simpson, R.L. A versatile sol-gel synthesis route to metal-silicon mixed oxide nanocomposites that contain metal oxides as a major phase. *J. Non-Crystalline Solids.* **350**, 173-181 (2004).
19. Gash, A.E., *et al.* Use of epoxides in the sol-gel synthesis of porous iron (III) oxide monoliths from Fe(III) salts. *Chem. Mater.* **13**, 999-1007 (2001).

